Tunable *in-situ* electro-polymerization of hydrogel films for microchip-based bioanalysis

Nan Shi and Victor M. Ugaz[a)]
Artie McFerrin Department of Chemical Engineering, Texas A&M University, College Station, Texas 77843-3122, USA

(Received 3 February 2016; accepted 11 May 2016; published online 26 May 2016)

Electro-polymerization phenomena have been previously investigated at the macroscale in the context of producing polymeric coatings over extended surface areas. But electrical actuation also offers exquisite local control of the polymerized films' position, morphology, and thickness, suggesting compelling advantages in microfluidic-based analysis systems. Here, we introduce a microfabricated platform incorporating arrays of individually addressable on-chip electrodes capable of generating discretely positioned electro-polymerized hydrogel films inside microchannels in timescales of ~5 min. Sequential actuation of specific electrode pairs initiates localized propagation of anchored polyacrylamide gel films and permits directed control of their size, shape, and growth rate. In addition to precise positioning of hydrogel films, obstacles, and barriers within microchannel networks, our approach makes it possible to encapsulate macromolecules within the films during polymerization, suggesting utility in a host of areas including separations, sample purification, and immunoassays. *Published by AIP Publishing*. [http://dx.doi.org/10.1063/1.4952420]

INTRODUCTION

The ability to synthesize polymer films anchored to solid surfaces is important in a wide range of areas including sensing,[1,2] construction of scaffolding or primer layers for biological analysis,[3,4] and protection/passivation of corrodible surfaces.[5,6] Conventional chemically initiated polymerization is generally employed to produce these coatings, but electro-polymerization methods whereby the reaction is electrochemically catalyzed offer intriguing advantages. Many standard reagent mixtures contain inherently electro-decomposable species that can produce free radicals upon application of a relatively small potential, whereas the purely chemical approach requires the use of additional reagents to initiate polymerization.[7] More importantly, electrical actuation introduces the possibility to start and stop the polymerization reaction in discrete increments so that a fine level of control can be exerted over the thickness and properties of the generated film. Previous studies have recognized these potential advantages and explored them in the context of thin film polymerization on macro-scale electrode surfaces.[8–10] But only a relatively limited range of reagent formulations and electrode metals have been considered.

Recent advancements in microscale chemical and biochemical analysis systems have sparked new interest in methods capable of controllably embedding polymer films within enclosed microchannel environments. These needs, combined with the ability of conventional microfabrication technology to construct precisely patterned micron-scale electrode arrays within microchannel networks, have motivated us to re-examine electro-polymerization as a potential enabling tool. Here, we show how electro-polymerization can be exploited to controllably embed crosslinked polyacrylamide gel films inside microchannels. The position, size, and shape of the polymerized films can be broadly controlled by modulating the governing

[a)]Author to whom correspondence should be addressed. Electronic mail: ugaz@tamu.edu. Telephone: +1 (979) 458-1002. Fax: +1 (979) 845-6446.

electrochemical processes localized in the vicinity of the electrode surfaces. We also demonstrate the ability of these films to function as obstacles for size-based fractionation of analytes and to locally embed macromolecular-sized species for applications involving encapsulation and delivery.

MATERIALS AND METHODS

Reagents and materials

Electro-polymerization studies were performed using monomer concentrations typically employed for gel electrophoresis (6%T and 2.5%C, diluted from a 30%T stock solution of Duracryl polyacrylamide sequencing gel (Proteomic Solutions)). Microspheres of average diameter 10 and 20 μm (2.74% and 2.52% solid-latex, respectively) were obtained from Polysciences, quantum dot nanoparticles (Qdot 525 streptavidin conjugate; 1 μM, borate buffer, pH 8.3; 0.5 μM concentration in polymerization solution) were acquired from Invitrogen, and fluorescein isothiocyanate (FITC) labeled bovine serum albumin (BSA) was obtained from Sigma-Aldrich (Cat. No. A9771; 1.5 mg/5 ml concentration in polymerization solution). Tris-borate-EDTA (TBE) buffer (Extended Range, Cat. No. 161–0741) and ammonium persulfate (APS) (Cat. No. 161-0700) were acquired from Bio-Rad Laboratories. FITC labeled biotin was purchased from AnaSpec, Inc. (Cat. No. 60654), streptavidin conjugated acrylamide was obtained from Life Technologies Corporation (Cat. No. 60654), and K_2SO_4 was obtained from Sigma-Aldrich (Cat. No. 221325).

Experiment protocol

Reagents were injected into the microchannels using a syringe, after which a pair of neighboring electrodes in the array was selected to function as the anode and cathode. A 2.5 V potential was applied across the electrode pair for timescales ranging from 1 to 10 min, after which the potential was switched off and the remaining unreacted monomer solution was removed. The microchannels were then rinsed 2–3 times with 0.5× TBE buffer before acquiring bright field images of both electrodes (TBE buffer was diluted to the desired concentration from a 10× stock solution). Phenomena within the microfluidic networks were imaged using a Zeiss Axioskop 2 microscope with a long working distance 10× objective. Illumination was achieved using a HBO 100 mercury arc lamp with FITC filter set, and image acquisition was performed using an ORCA-ER CCD camera (Hamamatsu).

RESULTS AND DISCUSSION

Mechanism and control of electro-polymerization

We employed a microdevice design previously described for microchip gel electrophoresis[11,12] incorporating arrays of platinum electrodes patterned on the surface of a silicon substrate (50 μm wide, 225 μm spacing between adjacent electrodes). An etched glass microchannel (300 × 50 μm cross-sectional dimensions) was bonded to the silicon substrate using UV-curable adhesive (SK-9 Lens Bond, Summers Optical) to create enclosed microchannels with electrodes extending across the floor (Figure 1(a)). Positions of the polymerized films (anode vs. cathode) obtained using different reagent compositions are summarized in Table I. Solutions containing only APS and monomer (6%T, 2.5%C) predominantly generate films on the cathode (Figure 1(b)). No change in position was observed upon addition of 0.5× TBE buffer to the monomer solution, but increasing the buffer concentration to 2× and 5× shifted the film from the cathode to the anode surface (Figure 1(c)). The effect of salt concentration was evaluated by addition of K_2SO_4, which maintained the polymer film at the cathode surface over the concentration range tested (0.01 to 0.1M). These observations suggest the following general mechanism to explain the associated electrochemical reactions (Figure 1(d)):

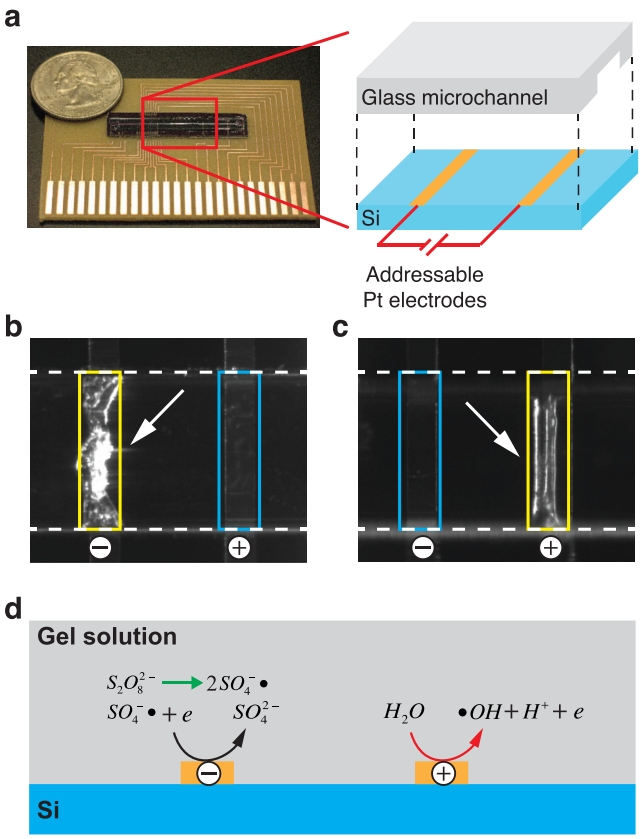

FIG. 1. Electro-polymerization of anchored hydrogel films. (a) Left: Microdevice assembly consisting of a silicon substrate containing patterned platinum electrode arrays bonded to an etched glass microchannel. The device is affixed to a printed circuit board and mounted on a microscope stage to enable visualization of the polymerized films. Right: Expanded schematic showing electrode placement within the microchannel. The microchannel is 1.5 cm long with cross sectional dimensions of $300 \times 50\ \mu$m. The electrodes are $50\ \mu$m wide with an edge-to-edge spacing of $225\ \mu$m between anode and cathode. The electrodes extend across the floor of the microchannel to ensure uniformity of the electric field under an applied potential. (b) Bright field image showing a hydrogel film polymerized at the cathode when the reagent mixture contains acrylamide, crosslinker, and APS. (c) Addition of 2× TBE buffer shifts the polymerized film to the anode. Monomer concentrations of 6%T, 2.6%C and an APS concentration of 0.1M were used in both (b) and (c). A 2.5 V potential was applied for 10 min. Yellow boxes indicate gel film position, blue boxes denote counter-electrode, and dashed white line denotes microchannel sidewalls. (d) Competitive reaction pathways involving radical species explain gel film polymerization at different electrodes. In the absence of TBE, the rate of radical formation at the cathode (green arrow) is faster at the cathode than at the anode (red arrow). As the solution's buffering capacity is increased by addition of TBE, the rate of anodic decomposition of water into hydroxyl radicals increases, also increasing the deactivation of radicals of $SO_4^{-}\bullet$, favoring polymerization at the anode. Scale: electrodes are $50\ \mu$m wide.

TABLE I. Influence of reagent composition on location of electro-polymerized gel films.

Reagent composition	Gel film location
6%T + 2.6%C, 0.1M APS	Cathode
6%T + 2.6%C, 0.1M APS, 0.5× TBE	Cathode
6%T + 2.6%C, 0.1M APS, 2× TBE	Anode
6%T + 2.6%C, 0.1M APS, 5× TBE	Anode
6%T + 2.6%C, 0.1M APS, 0.01M K_2SO_4	Cathode
6%T + 2.6%C, 0.1M APS, 0.1M K_2SO_4	Cathode
6%T + 2.6%C, 0.1M APS, Quantum dots	Anode
6%T + 2.6%C, 0.1M APS, FITC-BSA	Cathode

Cathode

$$S_2O_8^{2-} \rightarrow 2SO_4^{-}\bullet$$
$$SO_4^{-}\bullet + e^- \rightarrow SO_4^{2-}$$
$$SO_4^{-}\bullet + monomers \rightarrow polymer$$
$$2SO_4^{-}\bullet + H_2O \rightarrow 2H^+ + 2SO_4^{2-} + \frac{1}{2}O_2$$

Anode

$$H_2O \rightarrow \bullet OH + H^+ + e^-$$
$$\bullet OH + monomers \rightarrow polymer$$
$$2\bullet OH \rightarrow H_2O + \frac{1}{2}O_2$$

In the cathodic reaction, persulfate ions quickly dissociate into radicals that then are either reduced to sulfate ions, initiate polymerization, or react with water. On the anodic side, hydroxyl radicals are slowly produced through electrolysis of water and quickly become depleted by side reactions.

When APS and monomer are the only components present in the reagent mixture, the cathodic reaction is expected to dominate because the fast timescale of persulfate ion dissociation is capable of both initiating polymerization and reacting with water to produce protons, thereby decreasing the local pH. These combined effects further slow down the anodic production of hydroxyl radicals, resulting in formation of the polyacrylamide film only at the cathode surface. Similarly, reduction of persulfate radicals is not favored when potassium sulfate is added based on the associated equilibrium constant for an elementary reversible reaction (i.e., $A + B \rightleftharpoons C$), providing an increased opportunity for these radicals to initiate polymerization. When TBE buffer is introduced into the reagent mixture, the film position moves from the cathode to the anode surface because protons generated from the anodic reaction are quickly neutralized as the solution's buffering capacity increases, thereby speeding up generation of hydroxyl radicals and electrons via water decomposition. These electrons, in turn, render the persulfate radicals at the cathode surface more easily reduced to ions so that fewer are available to initiate polymerization.

Several factors act simultaneously to create conditions favorable for localized polymerization within thin films anchored on the electrodes, as opposed to penetrating into the bulk of the microchannel. First, both the cathodic and anodic reactions only generate one unstable radical to initiate polymerization ($SO_4^{-}\bullet$ on cathode and •OH on anode), whereas multiple radicals are produced at the electrode surface in previous studies where formation of bulk gels was reported.[10] Second, oxygen produced by the electrode reactions can also act to neutralize radicals before they are able to initiate polymerization, further confining their activity. Finally, the electrode surface becomes covered by the growing gel film, establishing a barrier inhibiting transport of radicals from electrode surface toward the polymerization reaction front.

The cathodic and anodic reactions normally do not generate visible changes until at least 5 min of polymerization time has elapsed. Therefore, we estimate the approximate timescale for the reactions to be 5 min. It should be noted that in free solution, the diffusion of analytes (ions, radicals) would occur much faster. Assuming a diffusion coefficient of ions to be on the order of 10^{-10} m^2/s and taking the 50 μm electrode width as a typical length scale yields a time scale of order 10 s that is much less than the visually observed timescale for film formation. However, the process is also governed by diffusion through the growing polymer film, which occurs more slowly than in bulk. For example, assuming that the diffusion coefficient in the polymer film is 1/10 that in the bulk, then the resulting diffusion time will be on the order of minutes, which approaches the approximate timescale inferred by visual observation.

Polymerized film thickness

We obtained estimates of the gel film thickness by injecting solutions containing microspheres of known size and imposing a flow through the microchannel (Figure 2(a)). The polymerized film acts as a filter to block large microspheres, allowing only smaller sizes to travel downstream. The maximum size of microspheres that can pass over the film barrier is determined by the free space between the polymerized film surface (extending upward from the floor of the channel) and the ceiling of the microchannel. Since the channel height is known ($h_{channel} = 50\,\mu m$), the filter size cutoff ($d_{critical}$) is related to the film thickness (h_{film}) via $h_{film} = h_{channel} - d_{critical}$. In experiments involving microspheres with average diameters of 10

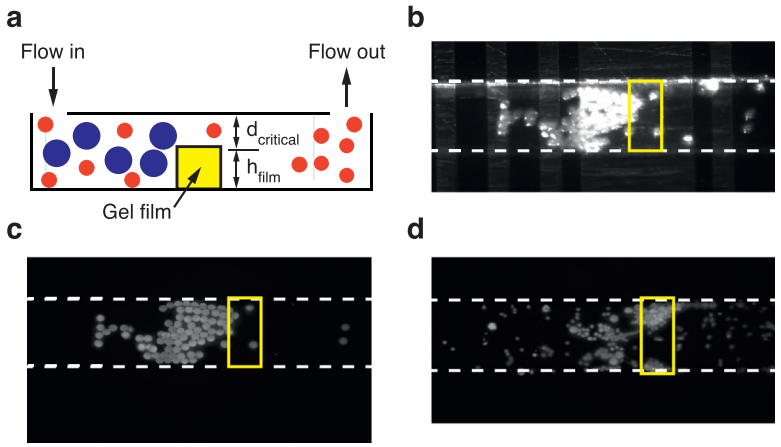

FIG. 2. Electro-polymerized gel film thickness. (a) Side-view schematic illustration of gel film geometry inside the microchannel, and its application as a barrier for species sized larger and smaller than $d_{critical}$ (not drawn to scale). After the film is polymerized at the electrode, unreacted monomer solution is removed and channel is rinsed with 0.5× TBE buffer. A solution containing microspheres with mixed sizes is then injected and a flow is imposed across the film. (b) Bright field and (c) fluorescence images of 20 μm diameter large microspheres show that they become blocked in front of the film interface. (d) A fluorescence image shows that 10 μm diameter microspheres are able to travel through the gap between the film and the microchannel ceiling. Microsphere solutions were diluted to 1/3 of the stock concentration. Scale: narrow electrodes are 50 μm wide (dashed lines). Flow direction is left to right; yellow box indicates gel film position; dashed white line denotes microchannel sidewalls.

and 20 μm, we observe that 10 μm microspheres freely travel past the film, while 20 μm microspheres are blocked at the gel interface (Figures 2(b)–2(d), polydispersity effects were not considered here, as size variations are less than 15% and 10% for the 10 and 20 μm beads, respectively, according to the manufacturer's data). Therefore, we estimate a film thickness of approximately 30–40 μm under the experiment conditions employed here.

Recalling that the films are formed via polymerization initiated by radicals generated at the surface of electrodes suggests general guidelines for selection of the governing parameters. Film thickness is expected to increase with increasing salt concentration and applied potential because both would generate more free radicals to initiate the polymerization. But the increased film thickness will eventually saturate at high salt concentration or potential because a fundamental transport limitation will be reached whereby radicals experience more diffusion resistance to reach the bulk solution. Additionally, the applied potential and buffer conductivity are constrained by the need to operate at relatively low potentials 1–2 V to remain below the threshold for gas bubble formation due to the electrochemical processes at the electrode surfaces.

Encapsulation of macromolecular and nanoparticle species

The 3D morphology of the electro-polymerized gel films provides a scaffold for localized biomolecule encapsulation because their position and size can be precisely controlled by adjusting reagent composition, applied potential, and electrode geometry. We explored this possibility by confining other species within the crosslinked polyacrylamide films during polymerization (Figure 3(a)). A reagent mixture containing the monomer/crosslinker mixture, APS, and either a macromolecule (FITC labeled BSA) or nanoparticle (quantum dot) additive was injected into the microchannel (Figures 3(b) and 3(c)). After applying a 2.5 V potential for 5 min, film formation could be observed under bright field imaging. The unreacted solution was removed, and the channel was rinsed several times with 0.5× TBE buffer to ensure that no free macromolecules or nanoparticles remained deposited on the surfaces of the channel or gel film. The embedded species were observed using a FITC filter set, revealing a homogeneous intensity inside the polymerized area localized at the electrode, dropping to zero outside the film boundary (our rinsing protocol ensured that the observed fluorescence was not due to surface affinity; however, this process also occasionally deformed the gel film interface, as evident in Fig. 3(b)). Intriguingly, we observe that the location of the polymerized films depends on whether the

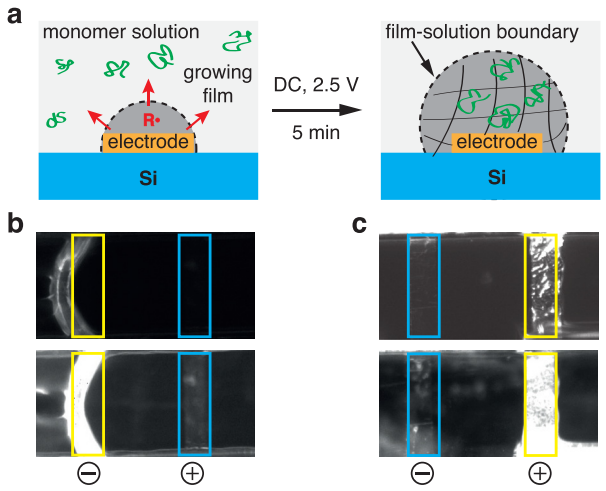

FIG. 3. Encapsulation of macromolecular and nanoparticle species. (a) Illustration of simultaneous film growth and macromolecule confinement during polymerization. (b) and (c) Bright field (upper panel) and fluorescence (lower panel) images reveal encapsulation of FITC-BSA and quantum dots, respectively. (b) FITC-BSA is encapsulated at the cathode and (c) quantum dots are encapsulated at the anode. The curved gel film in (b) emerges due to flow associated with removal of the unpolymerized monomer solution and subsequent rinsing buffer. Yellow boxes indicate gel film position; blue boxes denote counter-electrode. Scale: electrodes are 50 μm wide.

macromolecular or nanoparticle species is present during polymerization. The film containing BSA is synthesized on the cathode, whereas the quantum dot containing film appears on the anode. The position of the quantum dot containing film may be governed in part by the buffer formulation used to disperse the quantum dots, which has a pH value close to that of the 2× TBE buffer previously shown to yield film formation at the anode (Table I).

Embedded chemical functionality

To further demonstrate the ability of electro-polymerized films to function in scenarios pertinent to biological analysis, we added streptavidin functionalized acrylamide (final

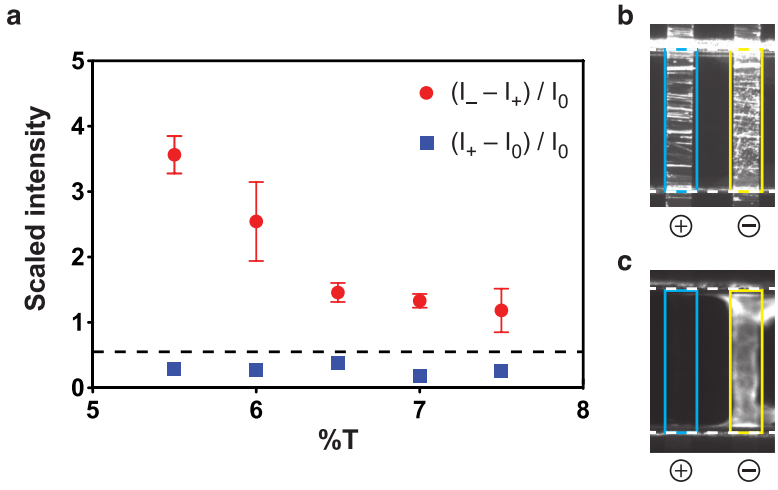

FIG. 4. Affinity capture within electro-polymerized gel films. (a) Fluorescence decreases with increasing acrylamide/bisacrylamide monomer concentration (red circles), indicating reduced biotin-streptavidin conjugation in denser gel networks. The quantities I_0, I_+, and I_- represent average intensity values associated with the background, cathode, and anode surfaces, respectively. Intensities observed at the unreacted electrode surface (blue squares) are lower than the anode in all cases. (b) Bright field and (c) fluorescence images reveal that affinity capture of species from the surrounding bulk flow is achieved in the electro-polymerized streptavidin-polyacrylamide gel films. Images were acquired after 3–5 min of incubation with FITC-biotin followed by rinsing with TBE buffer. Yellow boxes indicate gel film position; blue boxes denote counter-electrode; dashed white line denotes microchannel sidewalls. Scale: electrodes are 50 μm wide.

concentration 8 μM) into the gel precursor solution, which was prepared with different monomer concentrations (%T) but with fixed crosslinker composition (%C). After polymerization on the electrode, we injected a continuous flow of FITC labeled biotin (50 μM) to enable conjugation with the streptavidin embedded inside the gel film and finally rinsed the microchannel multiple times with 0.5× TBE buffer to wash away the unbound biotin. Compared with the unreacted electrode surface (anode), introduction of streptavidin into the electro-polymerized gel enables capture of the fluorescently labeled biotin, as evident by consistently high fluorescence intensity localized at the anchored film (Figure 4). These data indicate that the intensity decreases as the monomer concentration increases, likely reflecting the denser pore network produced in the hydrogel. These observations demonstrate a broad ability to tune both the density of encapsulated functional species and the rate of mass transfer within the nanoporous surroundings, creating a versatile platform for assays based on affinity and/or controlled release.

CONCLUSIONS

Electro-polymerization can be exploited at the microscale to synthesize hydrogel films with desired physico-chemical properties anchored at prescribed locations within a microchannel network. The position and size of the gel films can be precisely controlled by adjusting the reagent formulation (monomer/crosslinker, buffer, or salt concentrations) owing to the underlying reaction mechanism's interplay among pathways that direct radicals toward either initiation of polymerization or formation of inactive ions. Ultimately, it is of interest to determine the kinetics of film formation, its dependence on applied potential (magnitude, duration, DC vs. AC), and the impact of a superimposed flow. We did not address these parameters in the current study due to challenges associated with *in-situ* monitoring of the gel film during polymerization. Follow-up studies are underway to elucidate these details so that a more complete fundamental understanding can be obtained. However, we note that the body of existing literature dealing with electro-polymerization at the macroscale and its applications toward surface coatings and passivation (cited in the introduction) provides a useful starting point.

We also remark that the polymerized films are strictly localized at the surface of the electrodes, enabling guided patterning of both position and morphology. The ∼30 μm film thicknesses achieved in our preliminary studies span approximately half the microchannel height, allowing sufficient 3D volume for encapsulation of relatively large macromolecular species within the gel. Although a standard monomer system (acrylamide) is used here, considerable potential exists to expand functionality by grafting of functional groups or use of other polymer gel systems. The electric power needed to actuate polymerization is also small (∼2.5 V potential), making it possible to actuate the process using 2 ordinary AA-size batteries.

The applicability of our method as an enabling tool in microscale chemical and biochemical analysis systems is evident in the context of two potential application areas. First, immunoassays rely on constructing arrays of capturing species immobilized at a surface, often requiring multiple reaction steps (e.g., enzyme-linked immunosorbent assays (ELISAs)[13–15]). Electro-polymerization can enable these arrays to be precisely patterned by employing a starting monomer solution containing the desired chemical or physical moieties. A second example involves isoelectric focusing of proteins in microfluidic systems, where distinct spatial zones with fixed pH must be established to capture proteins based on their isoelectric points (pI).[16,17] Our method offers a pathway to address this need by employing monomers that contain buffering groups (e.g., immobilines[18] incorporating both double bonds for polymerization and weak acid or basic groups to maintain local pH). Films polymerized from these monomers would embed sufficient buffering power to maintain the local pH within a precisely determined range.

ACKNOWLEDGMENTS

V.M.U. gratefully acknowledges support from the U.S. National Science Foundation under Grant No. CBET-1160010 and 1605167 and the Camille & Henry Dreyfus Foundation.

[1]M. C. Blanco-Lopez, S. Gutierrez-Fernandez, M. J. Lobo-Castanon, A. J. Miranda-Ordieres, and P. Tunon-Blanco, "Electrochemical sensing with electrodes modified with molecularly imprinted polymer films," Anal. Bioanal. Chem. **378**, 1922–1928 (2004).
[2]G. Herlem, B. Lakard, M. Herlem, and B. Fahys, "pH sensing at Pt electrode surfaces coated with linear polyethylenimine from anodic polymerization of ethylenediamine," J. Electrochem. Soc. **148**, E435–E438 (2001).
[3]S. Cosnier, "Electropolymerization of amphiphilic monomers for designing amperometric biosensors," Electroanalysis **9**, 894–902 (1997).
[4]W. Schuhmann, "Conducting polymer based amperometric enzyme electrodes," Microchim. Acta **121**, 1–29 (1995).
[5]F. Deflorian, L. Fedrizzi, A. Locaspia, and P. L. Bonora, "Testing of corrosion resistant fluoropolymer coatings," Electrochim. Acta **38**, 1945–1950 (1993).
[6]J. W. Holubka, W. Chun, A. R. Krause, and J. Shyu, in *Polymeric Materials for Corrosion Control ACS Symposium Series*, edited by F. Floyd and R. A. Dickie (American Chemical Society, 1986), Chap. 17, pp. 194–202.
[7]S. N. Bhadani, Y. K. Prasad, and S. Kundu, "Electrochemical and chemical polymerization of acrylamide," J. Polym. Sci.: Polym. Chem. Ed. **18**, 1459–1469 (1980).
[8]J. Bunsow and D. Johannsmann, "Patterned hydrogel layers produced by electrochemically triggered polymerization," Macromol. Rapid Commun. **30**, 858–863 (2009).
[9]J. Reuber, H. Reinhardt, and D. Johannsmann, "Formation of surface-attached responsive gel layers via electrochemically induced free-radical polymerization," Langmuir **22**, 3362–3367 (2006).
[10]G. Yildiz, H. Çatalgil-Giz, and F. Kadirgan, "Electrochemically prepared acrylamide/N,N′-methylene bisacrylamide gels," J. Appl. Electrochem. **30**, 71–75 (2000).
[11]R. C. Lo and V. M. Ugaz, "Microchip DNA electrophoresis with automated whole-gel scanning detection," Lab Chip **8**, 2135–2145 (2008).
[12]F. A. Shaikh and V. M. Ugaz, "Collection, focusing, and metering of DNA in microchannels using addressable electrode arrays for portable low-power bioanalysis," Proc. Natl. Acad. Sci. U.S.A. **103**, 4825–4830 (2006).
[13]S. Edmondson, V. L. Osborne, and W. T. Huck, "Polymer brushes via surface-initiated polymerizations," Chem. Soc. Rev. **33**, 14–22 (2004).
[14]T. G. Henares *et al.*, "Novel fluorescent probe for highly sensitive bioassay using sequential enzyme-linked immunosorbent assay-capillary isoelectric focusing (ELISA-cIEF)," Analyst **138**, 3139–3141 (2013).
[15]R. M. Lequin, "Enzyme immunoassay (EIA)/enzyme-linked immunosorbent assay (ELISA)," Clin. Chem. **51**, 2415–2418 (2005).
[16]S. Jezierski, D. Belder, and S. Nagl, "Microfluidic free-flow electrophoresis chips with an integrated fluorescent sensor layer for real time pH imaging in isoelectric focusing," Chem. Commun. **49**, 904–906 (2013).
[17]S.-W. Tsai, M. Loughran, A. Hiratsuka, K. Yano, and I. Karube, "Application of plasma-polymerized films for isoelectric focusing of proteins in a capillary electrophoresis chip," Analyst **128**, 237–244 (2003).
[18]M. Chiari and P. G. Righetti, "The Immobiline family: From "vacuum" to "plenum" chemistry," Electrophoresis **13**, 187–191 (1992).